

Quantum three-body calculation of the nonresonant triple- α reaction rate at low temperatures

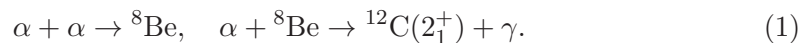
Kazuyuki OGATA^{1*)}, Masataka KAN^{1**)}, and Masayasu KAMIMURA^{1,2}

¹*Department of Physics, Kyushu University, Fukuoka 812-8581, Japan*

²*RIKEN Nishina Center, 351-0198 Wako, Japan*

The triple- α reaction rate is re-evaluated by directly solving the three-body Schrödinger equation. The resonant and nonresonant processes are treated on the same footing using the continuum-discretized coupled-channels method for three-body scattering. Accurate description of the α - α nonresonant states significantly quenches the Coulomb barrier between the two- α 's and the third α particle. Consequently, the α - α nonresonant continuum states below the resonance at 92.04 keV, i.e., the ground state of ^8Be , give markedly larger contribution at low temperatures than in foregoing studies. We show that Nomoto's method for three-body nonresonant capture processes, which is adopted in the NACRE compilation and many other studies, is a crude approximation of the accurate quantum three-body model calculation. We find about 20 orders-of-magnitude enhancement of the triple- α reaction rate around 10^7 K compared to the rate of NACRE.

After the Big Bang, all elements surrounding us have been created in the cosmos. Among them, ^{12}C is one of the most important nuclei because it is an essential element of life. In this sense, to understand the origin of ^{12}C would be equivalent to know “*where we come from.*” In view of nuclear physics, it is well known that the second 0^+ state of ^{12}C at 7.65 MeV above its ground state was predicted by Hoyle in 1953 to explain the abundance of ^{12}C , or, existing of human beings; this challenging prediction was soon confirmed experimentally,¹⁾ and the 0_2^+ state newly discovered is called the Hoyle resonance. Since this historic discovery of the Hoyle resonance, the $\alpha(\alpha\alpha, \gamma)^{12}\text{C}$ reaction, i.e., the so-called triple- α reaction, has been described as a series of the following two reactions:²⁾



In the latter, ^{12}C in the 2_1^+ state is formed by a γ -decay from the Hoyle resonance, and then decays into the ground state of ^{12}C , with emitting γ again. This picture of the triple- α reaction, which is realized at temperatures higher than a few 10^8 K in helium burning stars, successfully describes the present abundance of ^{12}C .

At low temperatures, however, the energy of the three α system cannot reach the resonance energy of 379.5 keV above the three- α threshold. A formation process through nonresonant three- α continuum states, i.e., the nonresonant triple- α process, then becomes dominant. The formation rate of ^{12}C at low temperatures is of crucial importance for studies on helium burning in accreting white dwarfs and neutron stars,^{3),4)} and is believed to strongly affect the evolution of primordial stars.⁵⁾ In Ref. 3) Nomoto proposed a method for evaluating contribution of the

*) E-mail: ogata@phys.kyushu-u.ac.jp

**) Present address: Advanced Information Systems R&D Department, Hitachi Ltd., Kawasaki 212-8567, Japan

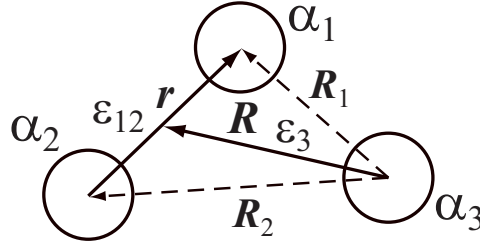
nonresonant triple- α process by using resonance formulae, with an *energy shift* for the Hoyle resonance, to describe the two reactions of Eq. (1). This method, which we call Nomoto's method in this Letter, was found to give a significantly larger triple- α reaction rate at low temperatures^{3),6)} than that obtained by a naive resonance formula without the energy shift. Nomoto's method has been a standard method for describing the nonresonant triple- α reaction. It should be noted, however, that Nomoto's method does not explicitly describe the role of the nonresonant continuum states in the triple- α process.

In the present Letter, we evaluate the nonresonant triple- α reaction rate by directly solving the Schrödinger equation of the three- α system. The three- α scattering wave function is obtained by the continuum-discretized coupled-channels method (CDCC),⁷⁾ which was proposed and developed by the Kyushu group more than 20 years ago, and has been successfully applied to studies of various three-body reaction processes; see, e.g., Refs. 7)–9). In CDCC, resonant and nonresonant states of the α - α system, as well as those of the three- α system, are treated on the same footing. This is one of the most important advantages of the present calculation.

As for previous three-body calculations of the triple- α reaction, Kamimura and Fukushima¹⁰⁾ firstly showed, using the microscopic three- α resonating group method, the importance of the couplings between the α - α resonant channel and the α - α nonresonant channels for reproducing the properties of the Hoyle resonance and understanding the processes of Eq. (1). This finding was confirmed by Descouvemont and Baye¹¹⁾ using the microscopic three- α generator coordinate method; they derived the triple- α reaction rate down to 10^7 K. In these studies, however, treatment of the α - α nonresonant continuum was very primitive; only a few discretized nonresonant states were included. More seriously, α - α nonresonant continuum states below the resonance at 92.04 keV, which play essential roles in the nonresonant triple- α process as shown below, were completely missed. Thus, it is obvious that these models cannot accurately describe the nonresonant triple- α process at low temperatures, say, $T \lesssim 10^8$ K.

CDCC is well known as one of the most accurate reaction models to describe three-body reactions. It works even cases where Coulomb interactions play dominant roles and careful description of low-energy continuum states is required. In the present study, we use the three- α scattering wave function obtained by CDCC, and evaluate the triple- α reaction rate at temperatures of 10^7 K $\leq T \leq 10^9$ K. Emphasis is on the reaction rate at low temperatures for $T \leq 10^8$ K, where contribution of the nonresonant triple- α process is dominant. We show that Nomoto's method^{3),6)} used in the NACRE compilation¹²⁾ and many other studies is a crude approximation of the accurate quantum three-body model calculation. At $T = 10^7$ K, typically, our new result is more than 20 orders-of-magnitude as large as that of NACRE.¹²⁾

In the present calculation, we work with the three- α system shown in Fig. 1 based on the Jacobi coordinates (\mathbf{r} , \mathbf{R}). The relative energy of α_1 and α_2 is denoted by ϵ_{12} and the relative energy between α_3 and the center-of-masses (c.m.) of α_1 and α_2 is denoted by ϵ_3 ; the total energy E in the three- α c.m. frame is $\epsilon_{12} + \epsilon_3$. We obtain the triple- α reaction rate by directly solving the following three-body

Fig. 1. Illustration of the three- α system.

Schrödinger equation:

$$[T_{\mathbf{r}} + T_{\mathbf{R}} + v(r) + v(R_1) + v(R_2) - E] \Psi(\mathbf{r}, \mathbf{R}) = 0, \quad (2)$$

where $T_{\mathbf{r}}$ and $T_{\mathbf{R}}$ are the kinetic energy operators associated with \mathbf{r} and \mathbf{R} , respectively, and v is the interaction between two- α 's consisting of the nuclear and Coulomb parts.

Following the standard continuum-discretization procedure called *the average method*,⁷⁾ we first discretize the continuum states of the α_1 - α_2 subsystem into momentum bins. We prepare L^2 -integrable α_1 - α_2 wave functions $\hat{u}_i(r)$ ($i = 1-i_{\max}$) by

$$\hat{u}_i(r) = \int_{k_i}^{k_{i+1}} f_i(k) u(k, r) dk / \left[\int_{k_i}^{k_{i+1}} |f_i(k)|^2 dk \right]^{1/2}, \quad (3)$$

where $u(k, r)$ is the α_1 - α_2 scattering wave function with the relative momentum k , and $f_i(k)$ is a weight function set to be a constant and the Breit-Wigner function for nonresonant and resonant bin states, respectively.⁷⁾ Normalization of $u(k, r)$ is defined by $\int u^*(k', r) u(k, r) dr = \delta(k' - k)$, which makes $\hat{u}_i(r)$ satisfy $\int \hat{u}_i^*(r) \hat{u}_j(r) dr = \delta_{ij}$. The average momentum (energy) of the i th bin state of the α_1 - α_2 system is denoted by \hat{k}_i ($\hat{\epsilon}_{12,i}$) in the following. The total wave function of the three- α system with CDCC is given by

$$\Psi_{\hat{k}_{i_0}, E}^{0+}(r, R) = \sqrt{\frac{2}{\pi}} \frac{1}{32\pi^2} \frac{1}{\hat{k}_{i_0} \hat{K}_{i_0}} \sum_{i=1}^{i_{\max}} \frac{\hat{u}_i(r)}{r} \frac{\hat{\chi}_i^{(i_0)}(R)}{R},$$

where $\hat{\chi}_i^{(i_0)}(R)$ describes the relative motion between (α_1 - α_2) in \hat{u}_i and α_3 with the relative momentum \hat{K}_i that is obtained by energy conservation of the three- α system. The index i_0 represents the incident channel. Note that we consider only the s-waves of \hat{u}_i and $\hat{\chi}_i^{(i_0)}(R)$, since we are interested in a reaction at very low energies. Furthermore, we have dropped all phase factors in $\Psi_{\hat{k}_{i_0}, E}^{0+}$ giving no contribution to the reaction probability shown below. The coupled-channel (CC) equations for $\hat{\chi}_i^{(i_0)}(R)$ ($i = 1-i_{\max}$) are given by

$$[T_R + V_{ii}(R) - (E - \hat{\epsilon}_{12,i})] \hat{\chi}_i^{(i_0)}(R) = - \sum_{i' \neq i} V_{ii'}(R) \hat{\chi}_{i'}^{(i_0)}(R), \quad (4)$$

which are solved under a usual boundary condition for $\hat{\chi}_i^{(i_0)}(R)$.⁷⁾ The coupling potential $V_{ii'}(R)$ is defined by

$$V_{ii'}(R) = \left\langle \frac{\hat{u}_i(r)}{r} \left| v(R_1) + v(R_2) \right| \frac{\hat{u}_{i'}(r)}{r} \right\rangle_{\mathbf{r}}. \quad (5)$$

The reaction probability $\langle \sigma v \rangle_{\hat{k}_{i_0}, E}$ of the triple- α process due to the electric quadrupole (E2) transition to the 2_1^+ state is given by

$$\langle \sigma v \rangle_{\hat{k}_{i_0}, E} = \frac{2(2\pi)^7}{75\hbar} \left(\frac{\hbar\omega}{\hbar c} \right)^5 \sum_M \left| \langle \Psi_M^{2^+} | O_M^{\text{E2}} | \Psi_{\hat{k}_{i_0}, E}^{0^+} \rangle \right|^2,$$

where $\Psi_M^{2^+}$ is the wave function of the 2_1^+ state of ^{12}C with M the projection of the total spin, O_M^{E2} is the E2 transition operator, and the photon energy $\hbar\omega$ is given by $2.8358 + E$ MeV. Note that we use the symbol $\langle \sigma v \rangle$ for the reaction probability following NACRE;¹²⁾ it is actually the E2 transition probability divided by the normalization factor $1/(2\pi)^6$ for the three- α scattering wave function in free space. The triple- α reaction rate $\langle \alpha\alpha\alpha \rangle(T)$, as a function of T , is obtained by taking an average of $\langle \sigma v \rangle_{\hat{k}_{i_0}, E}$ with the Maxwell-Boltzmann distribution for the velocity of each α :

$$\langle \alpha\alpha\alpha \rangle(T) = 3N_{\text{A}}^2 \frac{4}{\pi (k_{\text{B}}T)^3} \int \left\{ \sum_{i_0=1}^{i_{\text{max}}} w_{i_0} \langle \sigma v \rangle_{\hat{k}_{i_0}, E} \right\} \exp\left(-\frac{E}{k_{\text{B}}T}\right) dE \quad (6)$$

with

$$w_{i_0} = \frac{2\hat{\epsilon}_{12, i_0}}{\hat{k}_{i_0}} \sqrt{\hat{\epsilon}_{12, i_0}(E - \hat{\epsilon}_{12, i_0})},$$

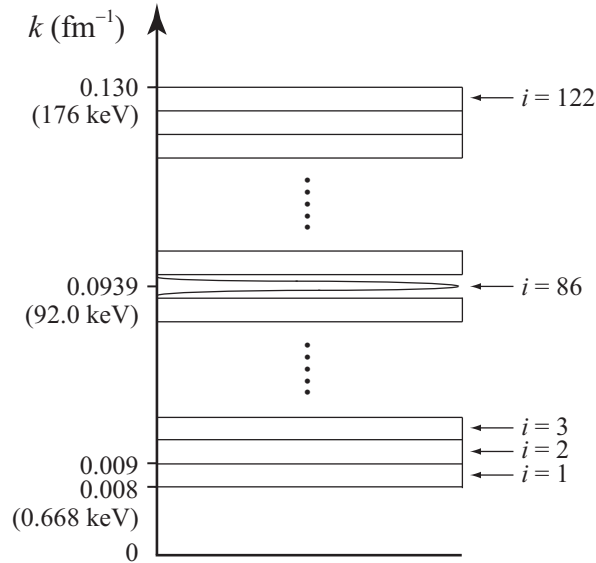


Fig. 2. α_1 - α_2 momentum bin states included in the present CDCC calculation.

where k_B is Boltzmann's constant and N_A is Avogadro's number. Factor 3 in Eq. (6) comes from the fact that the three- α system is symmetric with respect to an exchange of each pair of alpha particles.¹²⁾

In numerical calculation, we discretize the k -continuum of the α_1 - α_2 system from 0.008 fm^{-1} ($\epsilon_{12} = 0.668 \text{ keV}$) to 0.130 fm^{-1} ($\epsilon_{12} = 176 \text{ keV}$) with the width of 0.001 fm^{-1} , which results in $i_{\max} = 122$. Schematic illustration of the α_1 - α_2 bin states taken in the CDCC calculation is shown in Fig. 2. This discretization is sufficiently precise for the present purpose. The 86th bin corresponds to the α_1 - α_2 resonance. The maximum value of r is 5,000 fm with the increment Δr of 0.1 fm.

As for the nuclear potential between two α 's, we use the following two-range Gaussian form (with depth in unit of MeV):

$$v^{\text{nucl}}(x) = 100.0e^{-(x/1.00)^2} - 30.35e^{-(x/2.13)^2}, \quad (7)$$

where x is the displacement of the two α 's in fm. The first repulsive part simulates the Pauli exclusion principle that nucleons in an α cannot occupy the nucleon s-orbit in the other. This potential gives α - α resonance at 92.0 keV with the width of 4.8 eV, which reproduce well the corresponding experimental values, i.e., $92.04 \pm 0.05 \text{ keV}$ and $5.57 \pm 0.25 \text{ eV}$.¹³⁾ It is known¹⁴⁾ that this type of α - α potential with a repulsive core is not suitable for describing the 0_1^+ or 2_1^+ state of ^{12}C , in which the three- α particles are closely bound. However, it can successfully be applied to the 0_2^+ state, in which the three- α 's are loosely coupled. Therefore, we consider that the simulation of the Pauli principle by introducing the repulsive part is justified in describing the three- α scattering states. In fact, it is numerically confirmed that even if we put $v^{\text{nucl}}(x) = 0$ in the calculation of $V_{ii'}(R)$ given by Eq. (5), the resulting reaction rate $\langle \alpha\alpha\alpha \rangle(T)$ for $T \leq 10^8 \text{ K}$ changes by only about 2% at most.

Equations (4) are numerically integrated up to $R_{\max} = 2,500 \text{ fm}$ with $\Delta R = 0.25 \text{ fm}$, and $\hat{\chi}_i^{(i_0)}(R)$ ($i = 1-i_{\max}$) are connected to usual asymptotic form. The total energy E is varied from 1 keV to 500 keV with $\Delta E = 1 \text{ keV}$; around the Hoyle resonance at $E = 379.5 \text{ keV}$, we put $\Delta E = 0.1 \text{ keV}$. In the evaluation of the coupling potentials $V_{ii'}(R)$ given by Eq. (5), we reduce v^{nucl} by 1.5% so that the $(\alpha_1$ - α_2)- α_3 system in the $i = 86$ channel, with $i_0 = 86$, forms a resonance at $\epsilon_3 = 287.5 \text{ keV}$.

In the calculation of Ψ_M^{2+} , use of the potential of Eq. (7) is not appropriate as mentioned above. Instead, we adopt a sophisticated three- α wave function^{15),16)} that was obtained on the basis of the orthogonality condition model¹⁷⁾ for describing the Pauli principle with the three- α particles symmetrized. In this semi-microscopic calculation, the α - α potential was derived by folding an effective nucleon-nucleon force¹⁸⁾ into the α -particle density.

We show in Fig. 3 the discretized continuum wave functions $\hat{u}_i(r)$ of the α_1 - α_2 system (upper panel) and the Coulomb parts of the diagonal coupling potentials $V_{ii}^C(R)$ (lower panel). We use logarithmic scale for the horizontal axis in each panel. The solid, dashed, and dotted lines correspond to the α_1 - α_2 continuum states with the average energies $\hat{\epsilon}_{12,i}$ of 38.2 keV ($i = 53$), 92.0 keV ($i = 86$), and 152 keV ($i = 113$), respectively. One sees that the resonant wave function has a dominant amplitude in the interaction region ($r \lesssim 10 \text{ fm}$), while the nonresonant wave functions have appreciable amplitudes only at larger r . This clear difference in $\hat{u}_i(r)$ drastically

affects $V_{ii}^C(R)$ as shown in the lower panel. One sees that the Coulomb barrier height $V_{ii}^C(R)$ for the α_1 - α_2 nonresonant bins is very much lower than for the resonant bin. Thus, α_3 can easily approach to the α_1 - α_2 system when α_1 - α_2 is in nonresonant states. This important feature has not been considered in preceding studies with Nomoto's method.

Figure 4 shows the calculated results of $\langle\sigma v\rangle_{\hat{k}_{i_0},E}$; to show the difference between the resonant and nonresonant results clearly, CC effects are not included here. The solid (dashed) line corresponds to $i_0 = 53$ (86). One sees that the solid line has a completely different energy dependence from that of the dashed line. The nonresonant reaction probability $\langle\sigma v\rangle_{\hat{k}_{i_0},E}$ is almost constant (in the scale of the vertical axis in Fig. 4) above $E \sim 70$ keV, and dominates the resonant one for $E \lesssim 200$ keV. Note that for $i_0 = 53$, $E = 70$ keV corresponds to $\epsilon_3 = 31.8$ keV that agrees well with the *quenched* Coulomb barrier height shown by the solid line in Fig. 3 (lower panel).

If we disregard unphysically the channel dependence of the coupling potentials $V_{ii'}(R)$ and take only the diagonal components, by using the following replacement:

$$V_{ii'}(R) \rightarrow V_{86,86}(R)\delta_{ii'}, \quad (8)$$

we can simulate the evaluation of $\langle\sigma v\rangle_{\hat{k}_{i_0},E}$ with Nomoto's method; note that the 86th bin corresponds to the α_1 - α_2 resonant state. This replacement of $V_{ii'}(R)$ in Eq. (4) makes the three- α system form a resonance when $\epsilon_3 = 287.5$ keV, independently of ϵ_{12} . In other words, when $\epsilon_{12} = 92.0 - \Delta\epsilon_{12}$ keV, the three- α system has a resonance at $E = 379.5 - \Delta\epsilon_{12}$ keV. This $\Delta\epsilon_{12}$ is nothing but the energy shift in Nomoto's method. The result for $i_0 = 53$ with Eq. (8) is shown by the dotted line in

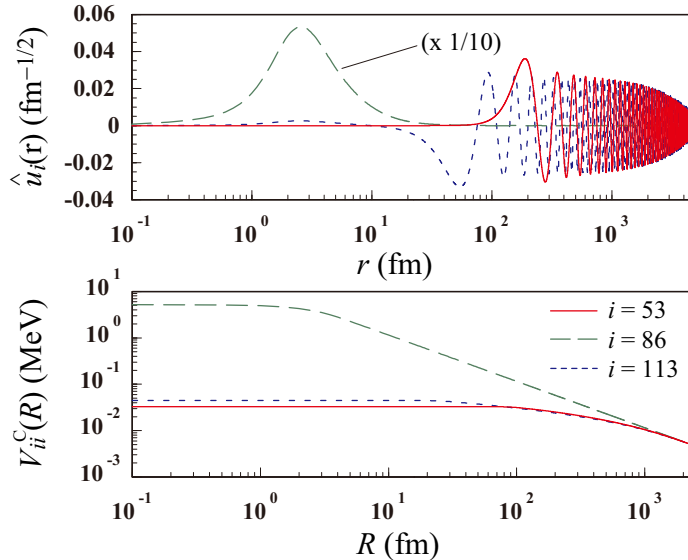


Fig. 3. (Color online) Discretized α_1 - α_2 continuum wave functions $\hat{u}_i(r)$ (upper panel) and the diagonal Coulomb potentials $V_{ii}^C(R)$ (lower panel). The solid, dashed, and dotted lines correspond to $i = 53, 86$ (resonance), and 113, respectively.

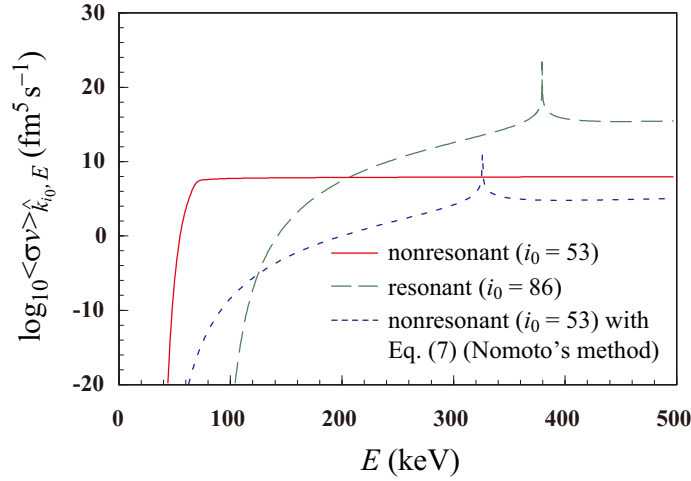


Fig. 4. (Color online) $\langle\sigma v\rangle_{\hat{k}_{i_0,E}}$ for $i_0 = 53$ (solid line) and $i_0 = 86$ (dashed line). The dotted line shows the result for $i_0 = 53$ with Eq. (8), which simulates Nomoto's method.

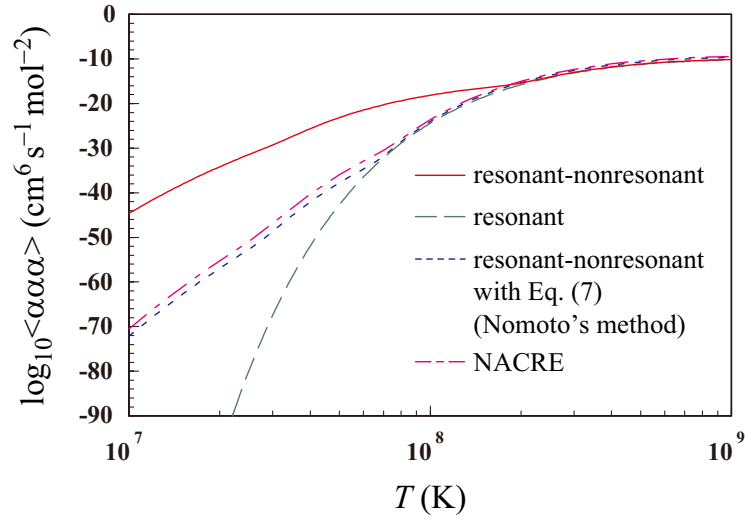


Fig. 5. (Color online) Triple- α reaction rate as a function of temperature. The solid line represents the result of CDCC. The dashed line shows the contribution of resonant capture. The result of CDCC simulating Nomoto's method with Eq. (8) is shown by the dotted line. The dash-dotted line shows the reaction rate of NACRE.¹²⁾

Fig. 4. Although it has a peak at $E \sim 326$ keV as expected, its energy dependence is similar to that of the dashed line, which results in a much smaller value than the *true* nonresonant capture probability (solid line) at low energies. Thus, Nomoto's method is shown to be a crude approximation of the accurate three-body model calculation.

We show by the solid line in Fig. 5 our result of the triple- α reaction rate obtained by CDCC. The triple- α reaction rate of the NACRE compilation¹²⁾ is shown by the dash-dotted line for comparison. Drastic enhancement of the reaction rate at low temperatures is found. The dashed line shows our result including only the resonant

capture process, i.e., via the $(\alpha_1\text{-}\alpha_2)\text{-}\alpha_3$ resonance state at $E = 379.5$ keV. Difference between the solid and dashed lines clearly shows the dominant contribution of the nonresonant triple- α process for $T \lesssim 2 \times 10^8$ K. As mentioned above, we can simulate the NACRE evaluation, which is essentially based on Nomoto's method, by using Eq. (8); the result of this calculation is shown by the dotted line. As expected, the dotted line reproduces well the result of NACRE. Thus, we conclude that the nonresonant capture process has much larger contribution than in previous evaluations,^{3), 6), 12), 19)} as a result of the significant reduction of the Coulomb barrier height between α_3 and the nonresonant $\alpha_1\text{-}\alpha_2$. This barrier reduction cannot be taken into account if one uses Eq. (8), or, equivalently, adopts Nomoto's method as mentioned above. Another remark is on the importance of the low-energy $\alpha_1\text{-}\alpha_2$ continuum states below the resonance at 92.04 keV, which were completely missed in the preceding three- α model studies.^{10), 11)} It is found that these low-energy states have almost all contributions to the total reaction rate (solid line) for $T \lesssim 4.0 \times 10^7$ K. Because of the lack of these states, the reaction rate given in Ref. 11), e.g., 5.34×10^{-63} $\text{cm}^6 \text{s}^{-1} \text{mol}^{-2}$ at 10^7 K, is markedly smaller than the present result at low temperatures.

Table I. The triple- α reaction rate (in $\text{cm}^6 \text{s}^{-1} \text{mol}^{-2}$) obtained by CDCC, together with its ratio to the rate of NACRE. The number $a[n]$ means $a \times 10^n$. Rates at other temperatures are available.

T (10^7 K)	$\langle\alpha\alpha\alpha\rangle$	ratio	T (10^7 K)	$\langle\alpha\alpha\alpha\rangle$	ratio
1	1.08[-44]	3.7[+26]	15	1.52[-16]	9.5[+01]
1.5	3.42[-38]	5.4[+23]	20	1.92[-15]	1.9[+0]
2	3.12[-34]	5.7[+21]	25	4.37[-14]	1.0[+0]
2.5	1.73[-31]	1.6[+20]	30	4.51[-13]	9.9[-1]
3	2.44[-29]	1.7[+18]	35	2.29[-12]	9.8[-1]
4	1.10[-25]	2.1[+15]	40	7.37[-12]	9.8[-1]
5	3.41[-23]	3.3[+13]	50	3.41[-11]	9.9[-1]
6	1.63[-21]	1.4[+12]	60	8.56[-11]	9.9[-1]
7	2.56[-20]	8.5[+10]	70	1.54[-10]	9.9[-1]
8	2.01[-19]	2.1[+09]	80	2.26[-10]	1.0[+0]
9	9.89[-19]	3.9[+07]	90	2.93[-10]	1.0[+0]
10	3.52[-18]	1.5[+06]	100	3.48[-10]	1.0[+0]

For more detailed comparison, we need renormalization for the CDCC result. We introduce an effective charge $\delta e = 0.77e$ to the E2 transition operator, so that our result of the $B(E2)$ value, evaluated at $E = 379.5$ keV with the 0^+ wave function normalized to unity, reproduces the experimental value of $13.4 e^2 \text{fm}^4$,²⁰⁾ just in the same way as in Ref. 11). Then, we renormalize our result (with δe) to the reaction rate of NACRE at $T = 10^9$ K, where the resonant capture process through the Hoyle resonance is dominant;¹²⁾ the renormalization factor obtained is 1.54. From this value, one may estimate the uncertainty of the present calculation to be more or less 50%.

In Table I we show the renormalized triple- α reaction rate obtained by CDCC, together with its ratio to the rate of NACRE, at some typical temperatures. As ex-

pected, for $T \geq 2.5 \times 10^8$ K the ratio is almost unity that shows our calculation, with the renormalization at 10^9 K, reproduces very well the temperature dependence of the resonant triple- α process through the Hoyle resonance. At low temperatures, on the other hand, the ratio exceeds 10^{20} , which will affect the helium burning in accreting white dwarfs and neutron stars. Furthermore, even at rather high temperature of 1.5×10^8 K, we obtain a larger reaction rate by almost two orders-of-magnitude than that of NACRE. It should be noted that a broad 2_2^+ resonance state at $E = 1.75$ MeV with the α -decay width of 0.56 MeV¹¹⁾ is included in the NACRE evaluation. In fact, it is shown that this 2_2^+ state has significant contribution to the triple- α reaction rate for $T \gtrsim 2 \times 10^9$ K.¹²⁾ At these high temperatures, the nonresonant triple- α process that we focus on in the present study will obviously be negligible compared to resonant processes via the 0_2^+ , 2_2^+ , and other possible resonance states⁵⁾ of ^{12}C . Very recently, it was reported²¹⁾ that a stellar evolution model computed with our new reaction rate of the triple α reaction caused inconsistency with observations of red giant branches. Further investigation on this implication will be very interesting and important.

In summary, we have evaluated the triple- α reaction rate by directly solving the three-body Schrödinger equation with CDCC. We treat the resonant and nonresonant processes on the same footing. The α - α continuum states below the resonance at 92.04 keV are shown to play essential roles in the nonresonant triple- α process for $T \lesssim 4.0 \times 10^7$ K. The key of the nonresonant capture process is that the Coulomb barrier between the two- α 's and the third α is much quenched compared to that in the resonant capture. This property extremely enhances the nonresonant triple- α process at low temperatures, i.e., $T \lesssim 10^8$ K. The ratio of our triple- α reaction rate to that of the NACRE compilation is more than 10^{26} at 10^7 K and about 100 at 1.5×10^8 K. It is found that Nomoto's method for three-body nonresonant capture processes, which is used in the NACRE compilation and many other studies, is a crude approximation, with Eq. (8), of the accurate quantum three-body model calculation. The newly evaluated triple- α reaction rate will affect many studies on nuclear astrophysics, those on helium burning in accreting white dwarfs and neutron stars in particular. Detailed description of the theoretical framework together with further discussion on the comparison with other existing methods will be presented in a forthcoming paper.

The authors wish to thank M. Kawai, M. Hashimoto, and E. Hiyama for helpful discussions.

-
- 1) D. N. F. Dunbar, R. E. Pixley, W. A. Wenzel, W. Whaling, Phys. Rev. **92** (1953), 649.
 - 2) C. Rolfs and H. P. Trautvetter, Annu. Rev. Nucl. Part. Sci. **28** (1978), 115.
 - 3) K. Nomoto, Astrophys. J. **253** (1982), 798.
 - 4) K. Nomoto, Astrophys. J. **257** (1982), 780.
 - 5) H. O. U. Fynbo *et al.*, Nature **433** (2005), 136.
 - 6) K. Nomoto, F.-K. Thielemann, and S. Miyaji, Astron. Astrophys. **149** (1985), 239.
 - 7) M. Kamimura, M. Yahiro, Y. Iseri, Y. Sakuragi, H. Kameyama and M. Kawai, Prog. Theor. Phys. Suppl. No. 89 (1986), 1.
 - 8) K. Ogata, S. Hashimoto, Y. Iseri, M. Kamimura and M. Yahiro, Phys. Rev. C **73** (2006),

- 024605.
- 9) J. A. Tostevin, D. Bazin, B. A. Brown, T. Glasmacher, P. G. Hansen, V. Maddalena, A. Navin, and B. M. Sherrill, *Phys. Rev. C* **66** (2002), 024607.
 - 10) M. Kamimura and Y. Fukushima, *Proceedings of the INS International Symposium on Nuclear Direct Reaction Mechanism*, Fukuoka, Japan, (1978) 409.
M. Kamimura, *Nucl. Phys.* **A351** (1981), 456.
 - 11) P. Descouvemont and D. Baye, *Phys. Rev. C* **36** (1987), 54.
 - 12) C. Angulo *et al.*, *Nucl. Phys.* **A656** (1999), 3.
 - 13) S. Wüstenbecker, H. W. Becker, H. Ebbing, W. H. Schulte, M. Berheide, M. Buschmann, C. Rolfs, G. E. Mitchell, and J. S. Schweitzer, *Z. Phys.* **A344** (1992), 205.
 - 14) H. Horiuchi, *Prog. Theor. Phys.* **51** (1974), 1266.
H. Horiuchi, *Prog. Theor. Phys.* **53** (1975), 447.
 - 15) E. Hiyama, M. Kamimura, T. Motoba, T. Yamada and Y. Yamamoto, *Prog. Theor. Phys.* **97** (1997), 881.
 - 16) E. Hiyama, Y. Kino, and M. Kamimura, *Prog. Part. Nucl. Phys.* **51** (2003), 223.
 - 17) S. Saito, *Prog. Theor. Phys.* **41** (1969), 705.
 - 18) A. Hasegawa and S. Nagata, *Prog. Theor. Phys.* **45** (1971), 1786.
 - 19) K. Langanke, M. Wiescher, and F.-K. Thielemann, *Z. Phys. A* **324** (1986), 147.
 - 20) F. Ajzenberg-Selove, *Nucl. Phys.* **A506** (1990), 1.
 - 21) A. Dotter and B. Paxton, arXiv:0905.2397 (2009).